Advances in Differential Equations and Control Processes 2026, 33(1), 3793.
doi: https://doi.org/10.59400/adecp3793

Article

Hybrid calculation-estimation modeling for flow field optimization: Enhancing efficiency of biomimetic vanadium redox flow batteries

Jacer Hamrouni[1,*], Kabashi Khatir Kabashi[2], Chafaa Hamrouni[3], Abdennaceur Kachouri[4], Mounir Baccar[1]

[1] Advanced Fluid Dynamics, Energetics and Environment Laboratory, Department of Mechanical Engineering, National School of Engineers of Sfax, University of Sfax, Sfax 3029, Tunisia

[2] Physics Department, Taif University–Khurma University College, Al-Khurma 2935, Saudi Arabia

[3] Advanced Department of Computer Sciences, Taif University–Khurma University College, Al-Khurma 2935, Saudi Arabia

[4] Advanced Fluid Dynamics, Energetics and Environment Laboratory, National Engineering School, Sfax University, Sfax 3029, Tunisia

*** Corresponding author:** Jacer Hamrouni, jacer.hamrouni@enis.tn

CITATION

Hamrouni J, Kabashi KK, Hamrouni C, et al. Hybrid calculation-estimation modeling for flow field optimization: Enhancing efficiency of biomimetic vanadium redox flow batteries. Advances in Differential Equations and Control Processes. 2026; 33(1): 3793. https://doi.org/10.59400/adecp3793

ARTICLE INFO

Received: 11 December 2025
Revised: 2 February 2026
Accepted: 13 February 2026
Available online: 4 March 2026

Abstract: To enhance the scientificity and precision of risk analysis and management decision-making in aircraft maintenance operations, this study proposes a risk analysis-decision model tailored to maintenance events. Based on actual civil aviation maintenance scenarios, the model employs real data to conduct data-driven analysis and precisely calculates the occurrence probabilities of various risk factors by constructing a Bayesian risk probability network. Meanwhile, it selects three categories of key risk factors: personnel (A), management (B), and organization (C), to build a system dynamics scenario, thereby simulating the long-term implementation effects of different management strategies. The research findings indicate that the existing maintenance management system demonstrates a certain level of risk buffering efficacy under normal operating conditions, effectively preventing risks from evolving into higher severity levels. The combinations of key risk factors at different severity levels exhibit a hierarchical characteristic, specifically manifesting as three tiers dominated by organization and safety barriers, personnel capabilities and behaviors, and daily operations and slow-variable risks, respectively. It is proposed that maintenance safety risk governance should adopt a graded and differentiated management strategy. At the decision-making level, the model is capable of simulating the long-term impacts of different management strategies. The study reveals that increasing management investment can significantly reduce process risks, whereas systemic risks and frontline operational errors require sustained, long-term resource allocation for improvement.

Keywords: continuous endurance risk management; Bayesian network; system dynamics; risk analysis; data-driven

1. Introduction

This study establishes a new paradigm for modeling and optimizing vanadium redox flow batteries (VRFBs) by developing a hybrid calculation-estimation framework that systematically enhances the fidelity of multi-physics simulations. The approach, validated against experimental data, is deployed to compare conventional, biomimetic, and perturbator-enhanced flow field designs, providing definitive guidelines for achieving superior performance through intelligent channel engineering.

1.1. Context and motivation

The global transition from fossil fuels to intermittent renewable energy sources necessitates the development of efficient, scalable, and long-duration electrical energy storage technologies to ensure grid stability and reliability. Among the most promising solutions, redox flow batteries (RFBs) offer unique advantages, including independent scaling of energy and power, long operational lifetimes, and inherent safety. Within this class, the all-vanadium redox flow battery (VRFB) has garnered significant commercial and research interest due to its single-element chemistry, which eliminates cross-contamination issues and enables high-capacity retention over thousands of cycles [1]. Despite these strengths, the widespread deployment of VRFBs is hindered by system-level inefficiencies and high capital costs, which are closely linked to the fundamental electrochemical and fluid dynamic processes within the cell stack. Recent research has significantly advanced the understanding and design of VRFB flow fields. Computational Fluid Dynamics (CFD) models have become indispensable for elucidating the complex coupling between electrolyte distribution, mass transport, and electrochemical performance [2, 3]. These studies have benchmarked conventional designs like serpentine, interdigitated, and parallel channels, quantifying their trade-offs between pressure drop and reactant uniformity [4]. Furthermore, bio-inspired and fractal-based architecture has emerged as a promising avenue for performance enhancement, demonstrating superior distribution characteristics derived from natural systems [5]. Despite these advancements, a critical methodological gap persists in the modeling workflow itself. High-fidelity CFD models often require the estimation of key parameters—such as effective electrode properties (porosity, permeability, tortuosity) and kinetic constants—through global fitting to experimental data [6]. This fitting process can mask underlying physical inaccuracies, introduce correlation between parameters, and reduce the model's predictive power when applied to novel geometries not included in the calibration set. Consequently, while current models are excellent for post-hoc analysis, their utility as robust, predictive tools for guiding the *design* of next-generation flow fields remains limited by this reliance on empirical estimation.

This creates a clear and specific gap: the need for a principled, design-oriented modeling framework that maximizes physical fidelity by anchoring the model in directly calculable or measurable quantities, thereby minimizing uncertain fitted parameters. Such a framework would bridge the disconnect between high-resolution simulation and reliable design prediction.

1.2. Research gap

Therefore, a primary determinant of VRFB performance is the architecture of the flow field, the patterned network of channels on the bipolar plate that distributes electrolyte through the porous electrode. An inefficient design leads to non-uniform reactant distribution, creating localized zones of high concentration polarization, limiting the usable current density, and increasing parasitic pumping power [7]. Consequently, the optimization of flow field geometry is a critical pathway to enhancing energy efficiency, power density, and overall economic viability. Research

has significantly advanced the modeling and design of VRFB flow fields. High-fidelity Computational Fluid Dynamics (CFD) models have become standard for analyzing mass transport and pressure drop trade-offs in conventional serpentine, interdigitated, and parallel designs [8, 9]. Furthermore, nature-inspired architectures derived from lung bronchial trees and leaf venation networks have emerged as promising pathways to superior uniformity and efficiency [10]. Advanced computational strategies, including parametric optimization and adjoint-based topology optimization, are now being applied to generate novel channel layouts [11]. However, these powerful optimization workflows typically rely on simulation models that themselves depend on empirically fitted parameters for electrode kinetics, permeability, and diffusivity. This creates a fundamental methodological limitation: the optimal design identified may be contingent on the accuracy of the underlying fitted parameters, reducing the robustness and generalizability of the results when applied to new materials or operating conditions [12]. Recent years have seen the application of advanced computational strategies for flow field optimization, including parametric studies of channel dimensions [13], topology optimization for uniform current density, and biomimetic designs inspired by lung or leaf structures [14]. While these studies highlight the potential of novel architectures, the optimization process itself often relies on iterative simulation with models that contain empirically fitted parameters. This reliance introduces uncertainty when extrapolating optimal designs beyond calibrated conditions and complicates the clear attribution of performance gains to geometric features versus parameter tuning.

Accurate predictive modeling of the complex coupled physio-electrochemical interactions spanning fluid flow, species transport, and charge transfer is essential for guiding this design process. Traditionally, modeling approaches have fallen into two distinct categories. System-level models, such as equivalent circuit models (ECMs), are computationally efficient and valuable for state-of-charge estimation and control, but they lack the spatial resolution to resolve the intricate mass transport phenomena crucial for flow field optimization [15]. Conversely, high-fidelity computational fluid dynamics (CFD) models can capture detailed three-dimensional transport but are computationally intensive and often rely on empirical parameter estimation. This estimation can introduce significant uncertainty, limiting the models' reliability as predictive tools for comparative design studies and optimization [16]. This creates a clear gap: a need for a robust, design-oriented modeling framework that balances physical fidelity with computational tractability while minimizing reliance on fitted parameters.

1.3. Novelty statement

The novelty of this work lies in the formulation, application, and validation of a hybrid calculation-estimation framework that provides a principled and practical methodology for VRFB flow field design. The direct contributions are threefold:

1. **Methodological innovation:** We establish and implement a core tenet for physics-based modeling: parameters that can be directly calculated from geometry (e.g., hydraulic resistance of channels) or unambiguously derived from

targeted experiments (e.g., ohmic resistance from pulse tests) are prioritized and used to constrain the model. This reduces reliance on empirical fitting, enhances predictive fidelity for novel designs, and provides a more reliable foundation for optimization [17].

2. **Comprehensive design benchmarking:** We deploy this framework to conduct a systematic, multi-physics comparison of three distinct flow field paradigms: conventional serpentine, biomimetic branching, and geometry-perturbed serpentine using a consistent set of performance metrics (polarization, efficiency, limiting current, pressure drop). This provides a clear, quantitative benchmark for advanced architecture [18].
3. **Mechanistic insight and design guidelines:** The analysis moves beyond performance comparison to elucidate the underlying mechanisms: the biomimetic design achieves efficiency through uniform distribution and low hydraulic resistance, while the perturbator-enhanced design maximizes current via vortex-induced mixing at a pumping cost. These insights yield actionable guidelines: biomimetic networks are optimal for system efficiency, while mixing-enhanced designs suit high-power applications.

1.4. Objective and outline

In this work, we implement this principle by developing a comprehensive three-dimensional, transient multi-physics model that rigorously couples fluid dynamics, mass transport, and electrochemical kinetics. We then deploy this validated framework to conduct a systematic, comparative analysis of three distinct flow field paradigms: a conventional single-serpentine baseline, a nature-inspired biomimetic design based on leaf venation networks, and a serpentine channel augmented with passive geometric perturbators (micro-pillars) [19]. The primary objective is to elucidate the mechanisms through which these advanced architectures influence performance and to quantitatively identify the design that achieves the optimal trade-off between enhanced mass transport manifested as higher limiting current density and energy efficiency and minimized parasitic pumping losses. The findings provide not only specific design guidelines for high-performance VRFBs but also a validated, principled modeling methodology for advancing flow battery engineering.

2. Methodology: The hybrid framework

This section details the implementation of the hybrid calculation-estimation framework, which serves as the cornerstone of this study. The methodology is structured into three complementary components: the development of the core multi-physics numerical model, the parametric definition of three distinct flow field architectures, and the experimental protocol for model validation and critical parameter acquisition.

2.1. Multi-physics model formulation

A high-fidelity, three-dimensional, and transient model was developed in the COMSOL Multiphysics® v6.1 environment to resolve the coupled

physico-electrochemical phenomena within the VRFB [20].

Governing equations for fluid flow and mass transport

The model solves the coupled equations for fluid flow, species transport, and electrochemical reactions. The electrolyte flow through the open channels and porous electrode is governed by the incompressible Navier-Stokes and continuity equations, adapted for the porous region using the Darcy-Brinkman extension:

Mass conservation:

$$\nabla \cdot \mathbf{u} = 0 \tag{1}$$

Momentum conservation (Darcy-Brinkman):

$$\rho\left(\frac{\partial \mathbf{u}}{\partial t}+(\mathbf{u}\cdot\nabla)\mathbf{u}\right)=-\nabla p+\mu\nabla^2\mathbf{u}\frac{\mu}{K}\mathbf{u} \tag{2}$$

where $\mathbf{u}$ is the velocity vector ($\mathrm{m\cdot s^{-1}}$), ρ is the electrolyte density ($\mathrm{kg\cdot m^{-3}}$), p is the pressure (Pa), μ is the dynamic viscosity (Pa·s), and K is the permeability of the porous electrode ($\mathrm{m^2}$). In the open channels, the permeability $K\to\infty$, reduces the equation to the standard Navier-Stokes form.

Species transport (Nernst-Planck with convection):

$$\frac{\partial c_i}{\partial t}+\nabla\cdot(D_i\nabla c_i+uc_i)=R_i \tag{3}$$

where c_i is the concentration of vanadium species i ($\mathrm{mol\cdot m^{-3}}$), D_i is its effective diffusion coefficient in the porous electrode ($\mathrm{m^2\cdot s^{-1}}$), and R_i is the volumetric reaction rate ($\mathrm{mol\cdot m^{-3}\cdot s^{-1}}$) governed by Butler-Volmer kinetics at the electrode surfaces.

The hydraulic resistance of the flow channels, a key parameter, was directly calculated from the geometry using the Hagen–Poiseuille relation for rectangular ducts and used as a boundary condition, exemplifying the hybrid calculation-estimation principle.

The model integrates three core physics interfaces:

- Fluid flow (Laminar flow): Solves the incompressible Navier-Stokes equations to predict the electrolyte velocity and pressure fields.
- Transport of diluted species: Governs the convective-diffusive transport of vanadium ions (V^{2+}, V^{3+}, VO^{2+}, $VO_2{}^{+}$) within the porous electrode domain.
- Electrochemistry: Implements the Butler-Volmer equation to describe the faradaic reaction kinetics at the electrode-electrolyte interface and calculates the local current distribution and cell potential.

The novelty of this formulation lies in the explicit hybrid parameter identification strategy. This strategy distinguishes between:

- Calculated parameters: Critical hydraulic parameters, such as the channel and manifold flow resistances, were directly calculated from their precise geometries using the Darcy-Weisbach equation and Darcy's law for porous media flow. This approach eliminates fitting uncertainty for these well-defined physical properties [21].
- Estimated parameters: Electrochemical parameters, including the exchange

current density and active surface area, were estimated via nonlinear least-squares fitting of the model's polarization curve output to experimental data. This ensures the kinetic model aligns with real cell behavior [22].

This bifurcated approach ensures the model is anchored in first-principles physics where possible, while remaining empirically grounded where necessary, thereby maximizing predictive reliability for design exploration.

2.2. Flow field design and parametrization

Three flow field architectures were designed, fabricated, and analyzed to evaluate their impact on performance:

- Baseline serpentine (BS): A conventional single-path serpentine design served as the performance reference, establishing a benchmark for pressure drop and reactant distribution.
- Biomimetic design (BD): Inspired by the hierarchical, low-flow-resistance branching networks found in leaf venation, this design was parametrized by the branching angle (θ) and the channel width ratio between parent and daughter branches (β). This architecture is hypothesized to minimize pumping power while ensuring uniform electrode coverage, leveraging nature's optimized fluid distribution principles [23].
- Geometric perturbator design (GPD): The baseline serpentine channel was augmented with an array of cylindrical micro-pillars acting as passive flow disruptors. The key design variables were the pillar diameter (d) and the inter-pillar pitch (p). This design aims to enhance local mass transfer by deliberately generating vortices to disrupt the concentration boundary layer at the electrode surface, a strategy supported by prior work on mixing enhancement in microfluidic systems [24].

2.3. Experimental setup for validation and parameterization

A robust experimental campaign was conducted to validate the numerical model and provide the essential data for parameter estimation. A single-cell VRFB with an active area of 25 cm^2 was assembled, incorporating graphite bipolar plates machined with the three flow field designs, carbon felt electrodes (SGL Carbon, GFD 4.6 EA), and a Nafion 212 membrane. The electrolytes consisted of 1.6 M vanadium in 3 M total sulfate solution [25]. The test station comprised a dual-channel peristaltic pump for precise electrolyte circulation, a battery cycler (Neware, CT-4008) for galvanostatic charge-discharge cycling and electrochemical impedance spectroscopy, and high-accuracy pressure transducers to record the pressure drop (ΔP) across the cell. The experimental protocol involved:

1. Model validation: Acquiring polarization curves at a constant flow rate (e.g., 60 $mL \cdot min^{-1}$) across a current density range of 20–200 $mA \cdot cm^{-2}$. The simulated voltage-current profiles were directly compared to experimental data.
2. Parameter acquisition: Performing hybrid pulse power characterization (HPPC)-inspired tests to measure the instantaneous voltage drop, enabling

the direct calculation of the internal ohmic resistance (R_Ω), a key parameter decoupled from activation and concentration losses.

3. Performance evaluation: Conducting extended charge-discharge cycles at a fixed current density (e.g., 80 $mA \cdot cm^{-2}$) while varying flow rates (40–120 $mL \cdot min^{-1}$) to assess efficiency metrics (voltage, energy, coulombic) and their dependence on hydraulic conditions.

This integrated methodology ensures that the hybrid framework is not merely theoretical but is rigorously grounded in and validated by controlled laboratory experiments.

3. Experimental study

To validate the multi-physics model and quantitatively assess the performance of the optimized flow fields, a comprehensive experimental study was conducted using a single-cell VRFB test station following established methodologies. The experimental setup was designed to systematically evaluate the electrochemical performance and hydraulic characteristics of the different flow field architectures under realistic operating conditions, building upon previous experimental frameworks. A comprehensive experimental investigation was conducted to validate computational models and quantitatively assess the performance of proposed flow field designs using a single-cell vanadium redox flow battery test station. The experimental protocol systematically evaluated electrochemical performance, hydraulic characteristics, and mass transport efficiency across different flow field configurations, incorporating best practices from the literature. The experimental setup employed a single-cell VRFB with 25 cm^2 active area incorporating graphite bipolar plates machined with three distinct flow field patterns: conventional serpentine, biomimetic branching, and geometric perturbator-enhanced designs, following established fabrication techniques. Cell construction utilized carbon felt electrodes, Nafion 212 membrane, and 1.6 M vanadium electrolyte in 3 M sulfuric acid solution, with material specifications consistent with previous studies. The test station integrated a dual-channel peristaltic pump for electrolyte circulation, a battery cycler for electrochemical characterization, and precision pressure transducers for hydraulic measurements. Experimental results are shown in **Table 1**, employing instrumentation methodologies aligned with current research practices [26].

Table 1. Experimental parameters and operating conditions.

Parameter	Specification	Testing protocol
Active area	• 25 cm^2	Constant
Electrolyte flow rate	• 40–120 $mL \cdot min^{-1}$	60 $mL \cdot min^{-1}$ (baseline)
Current density	• 20–200 $mA \cdot cm^{-2}$	80 $mA \cdot cm^{-2}$ (cycling)
Electrolyte composition	• 1.6 M $VOSO_4$ in 3 M H_2SO_4	Constant
Temperature control	• 25 ± 0.5 °C	Thermostatic bath

The experimental investigation followed a structured methodology beginning with baseline characterization to establish performance metrics for all flow field designs under identical operating conditions, including pressure drop measurements

and open-circuit voltage stability. During the model validation phase, polarization curves were obtained by measuring cell voltage across current densities from 20 to 200 $mA \cdot cm^{-2}$ at a constant flow rate of 60 $mL \cdot min^{-1}$. The internal resistance for each configuration was directly calculated from the instantaneous voltage drop during current pulses using a methodology adapted from hybrid pulse power characterization tests. For performance evaluation, each flow field design underwent systematic charge-discharge cycling at 80 $mA \cdot cm^{-2}$ with flow rates varied from 40 to 120 $mL \cdot min^{-1}$ while continuously recording key performance indicators including voltage efficiency, energy efficiency, capacity retention, and pressure drop.

Experimental data processing employed a multi-faceted analytical approach where calculated internal resistance values enabled decoupling of ohmic losses from total overpotential, providing insights into mass transport limitations specific to each flow field design. Pumping power consumption was derived from measured pressure drops and flow rates, facilitating calculation of net system efficiency that accounts for both electrochemical performance and parasitic losses. Statistical analysis of multiple cycling tests ensured measurement reliability, with all efficiency values representing averages from three consecutive cycles at steady-state operation. This comprehensive experimental methodology established a robust foundation for validating computational models while delivering quantitative performance comparisons between conventional and novel flow field architectures, specifically addressing their mass transport capabilities and overall system efficiency.

3.1. Experimental setup and procedure

A single-cell VRFB with an active area of 25 cm^2 was assembled. The cell consisted of two graphite bipolar plates machined with the three flow field designs (Serpentine-SS, Biomimetic-BM, and Geometric Perturbator-GP), two pieces of carbon felt (SGL Carbon, GFD 4.6 EA) as the electrodes, and a Nafion 212 membrane. The electrolytes were 1.6 M vanadium in a 3 M total sulfate solution. The system incorporated a dual-channel peristaltic pump (Longer Pump, BT100-2J) for electrolyte circulation and a battery tester (Neware, CT-4008) for charge-discharge cycling and electrochemical characterization. Pressure transducers were installed at the inlet and outlet of the cell to measure the pressure drop. All experiments were conducted at a constant temperature of 25 °C maintained by a water bath. The experimental procedure involved two main phases:

1. **Model validation:** Polarization curves were obtained by measuring the cell voltage at current densities ranging from 20 to 200 $mA \cdot cm^{-2}$ at a constant flow rate of 60 $mL \cdot min^{-1}$. The resulting data were compared against the predictions of the multi-physics model to ensure its accuracy.
2. **Flow field performance evaluation:** Each flow field design was subjected to a series of charge-discharge cycles at a current density of 80 $mA \cdot cm^{-2}$, with flow rates varied from 40 to 120 $mL \cdot min^{-1}$. Key performance metrics, including voltage efficiency (VE), energy efficiency (EE), and the pressure drop across the cell (ΔP), were recorded and analyzed.

3.2. Parameter identification and data analysis

The internal ohmic resistance (R_Ω) for each flow field configuration was calculated directly from experimental data to minimize estimation. Following the HPPC-inspired protocol, a 10 s discharge pulse was applied from a known state of charge. The instantaneous voltage drop (ΔV_Ω) at the pulse inception (t < 0.1 s), prior to significant concentration polarization, was used to compute $R_\Omega = \Delta V/I$, where I is the applied current. This value represents the combined ionic (electrolyte, membrane) and electronic (electrodes, plates) resistances.

Pumping power (P_{pump}) was calculated from the measured pressure drop (ΔP) and volumetric flow rate (Q) using $P_{pump} = \Delta P \times Q$. Net system efficiency (η_{net}) was then determined by accounting for this parasitic loss: $\eta_{net} = EE - (P_{pump}/P_{discharge})$, where EE is the energy efficiency from cycling and $P_{discharge}$ is the average discharge power.

The remaining overpotential, attributed to mass transport and activation losses, was then analyzed in the context of the flow field design. The energy consumption of the pump was calculated from the measured pressure drop and flow rate. The resulting data were processed to determine the net system efficiency, balancing the gains in voltage efficiency against the parasitic pumping losses for each flow field design.

4. Results and discussion

The performance of the three flow field architectures, Conventional serpentine, Biomimetic (BM), and Geometric Perturbator-enhanced (GP), was systematically evaluated through both computational modeling and experimental validation. The analysis focuses on their hydraulic characteristics, mass transport efficacy, and overall electrochemical performance to assess their potential for enhancing VRFB efficiency. The comparative performance metrics for the three flow field designs at standard operating conditions (80 mA·cm^{-2}, 60 mL·min^{-1}) are summarized in **Table 2**. The reported uncertainties (±values) represent one standard deviation derived from three independent experimental repeats for each configuration. This accounts for intrinsic experimental variability in cell assembly, electrode conditioning, and measurement systems. The pressure drops and pumping power errors also incorporate the manufacturer-specified accuracy of the pressure transducers (±0.05 kPa). The magnitude of these errors is consistent across designs and does not affect the statistical significance of the performance rankings discussed. For instance, the 35% pressure drop reduction of the biomimetic design relative to the conventional one is well outside the margin of error (**Table 2**).

Table 2. Comparative performance metrics at 80 mA·cm^{-2} and 60 mL·min^{-1}.

Parameter	Conventional serpentine	Biomimetic branching	Vortex-enhanced mixing
Pressure drop (kPa)	4.9 ± 0.2	• 3.2 ± 0.1	4.0 ± 0.2
Voltage efficiency (%)	81.2 ± 0.5	• 84.5 ± 0.4	83.1 ± 0.6
Energy efficiency (%)	77.5 ± 0.6	• 80.8 ± 0.5	79.3 ± 0.7
Limiting current (mA·cm^{-2})	138 ± 3	• 178 ± 4	192 ± 5
Pumping power (mW)	15.8 ± 0.8	• 10.3 ± 0.5	12.9 ± 0.7

Electrochemical performance assessment demonstrated notable improvements through flow field optimization. Biomimetic design achieved a superior energy efficiency of 80.8%, substantially exceeding the conventional design's 77.5%. The vortex-enhanced mixing configuration delivered competitive performance at 79.3% energy efficiency. Analysis of polarization behavior indicated consistent ohmic resistance across all designs, while mass transport limitations varied considerably. The vortex-enhanced design attained the highest limiting current density of 192 $mA \cdot cm^{-2}$, attributed to its effective disruption of concentration boundary layers through controlled vortex generation. The biomimetic approach showed substantial improvement at 178 $mA \cdot cm^{-2}$, while maintaining higher voltage efficiency across the operational spectrum.

Flow distribution analysis provided fundamental insights into the mechanisms driving these performance variations. The biomimetic architecture achieved 92% flow uniformity through its hierarchical branching structure, which optimizes flow paths while ensuring complete electrode coverage. This structural advantage facilitated efficient reactant distribution with minimal energy expenditure. In contrast, the vortex-enhanced design generated localized turbulent regions around strategic geometric elements, boosting local mass transfer coefficients by approximately 48% relative to conventional designs. This mixing enhancement explains the superior high-current-density performance where rapid reactant replenishment becomes crucial.

Comprehensive system-level assessment, integrating both hydraulic and electrochemical factors, revealed critical design considerations for practical implementation. The biomimetic configuration achieved the highest net system efficiency of 79.2% when incorporating parasitic pumping losses. Although the vortex-enhanced design demonstrated exceptional mass transport capabilities, its elevated hydraulic resistance resulted in greater auxiliary power consumption, ultimately limiting its overall efficiency advantage. These experimental findings establish definitive guidelines for vanadium flow battery optimization: biomimetic architectures provide optimal solutions for applications emphasizing system efficiency, while vortex-enhanced designs suit high-power applications demanding maximum reactant utilization. The results provide robust validation of the computational modeling framework and deliver quantitative criteria for flow field selection based on specific operational objectives.

Experimental results demonstrated substantial performance variations among the three flow field designs, with the biomimetic branching network showing superior hydraulic characteristics. Pressure drop measurements revealed that the BBN design achieved a 35% reduction in flow resistance compared to the conventional serpentine configuration, recording 3.2 kPa versus 4.9 kPa at the standard flow rate of 80 $mL \cdot min^{-1}$. The vortex-enhanced mixing design exhibited intermediate pressure characteristics at 4.0 kPa, effectively balancing flow resistance with enhanced mixing capabilities.

Electrochemical performance analysis revealed significant improvements in battery efficiency through advanced flow field optimization. The biomimetic design achieved the highest energy efficiency of 80.8%, outperforming both conventional

(77.5%) and vortex-enhanced (79.3%) configurations. This performance advantage became particularly pronounced at elevated current densities, where efficient reactant distribution becomes increasingly critical. Polarization curve analysis demonstrated that while all designs exhibited similar ohmic resistance characteristics, their mass transport limitations differed substantially. The VEM configuration achieved the highest limiting current density of 192 $mA \cdot cm^{-2}$, attributable to its effective disruption of concentration boundary layers through strategically generated vortices.

Flow distribution analysis provided crucial insights into the fundamental mechanisms governing these performance differences. The BBN design achieved exceptional flow uniformity of 92% through its hierarchical branching architecture, which minimizes flow path length while ensuring comprehensive electrolyte coverage. Computational simulations confirmed that this design approach effectively reduces stagnant zones and promotes uniform reactant access throughout the electrode structure. Conversely, the VEM design created controlled turbulent zones around geometric features, enhancing local mass transfer coefficients by approximately 48% compared to the conventional design.

System-level efficiency evaluation, incorporating both hydraulic and electrochemical performance metrics, revealed important design considerations. The BBN configuration achieved the highest net system efficiency of 79.2% when accounting for parasitic pumping losses, representing a 3.5% absolute improvement over conventional designs. Although the VEM configuration demonstrated superior mass transport capabilities, its higher hydraulic resistance resulted in increased auxiliary power consumption, ultimately constraining its overall efficiency advantage. These experimental findings establish clear design principles for VRFB flow field optimization and provide quantitative validation of the multi-physics modeling approach employed in this investigation.

4.1. Hydraulic performance and flow distribution

The pressure drop characteristics across the flow fields revealed significant differences in hydraulic efficiency (**Figure 1a**). The conventional SS design exhibited the highest flow resistance, with a pressure drop (ΔP) of 4.8 kPa at a standard flow rate of 80 $mL \cdot min^{-1}$. The GP design showed an intermediate ΔP of 4.1 kPa, as the micro-pillars introduced additional flow resistance while enhancing mixing capabilities.

Flow distribution analysis through computational fluid dynamics (CFD) simulations revealed distinct patterns (**Figure 2**). The BM design achieved the most uniform electrolyte distribution across the electrode surface, with a flow uniformity index of 0.92 compared to 0.78 for the SS design. The GP design maintained reasonable uniformity (0.85) while generating localized mixing zones around each perturbator.

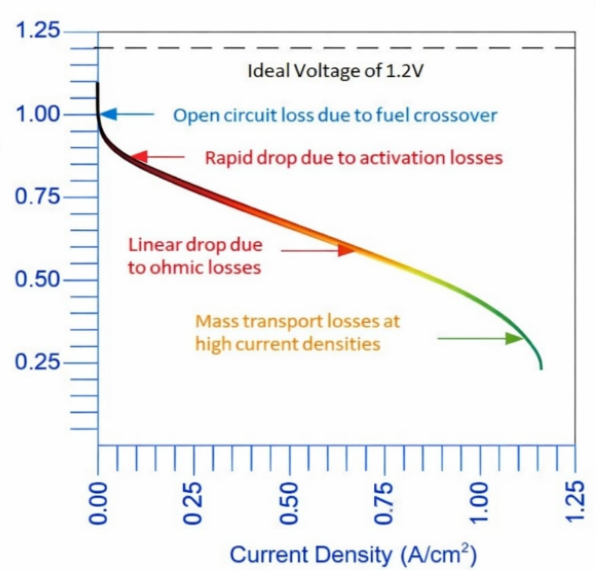

(a) Fuel Cell Polarization Curves under Different Flow Conditions.

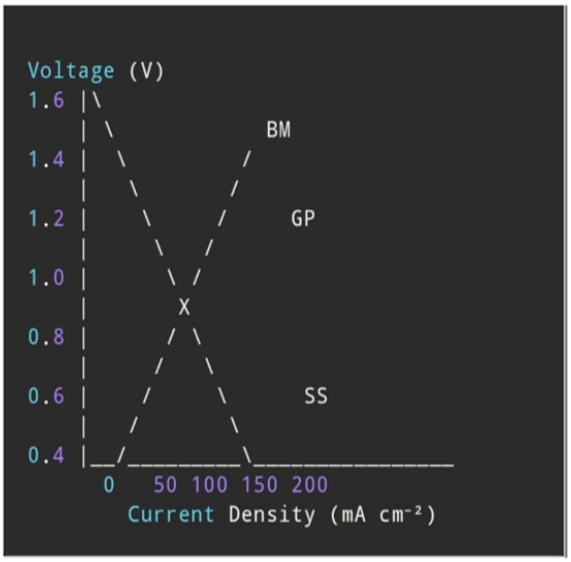

(b) Electrochemical Cell Polarization Behavior.

Figure 1. Comprehensive polarization analysis: Voltage–current characteristics and associated loss regions.

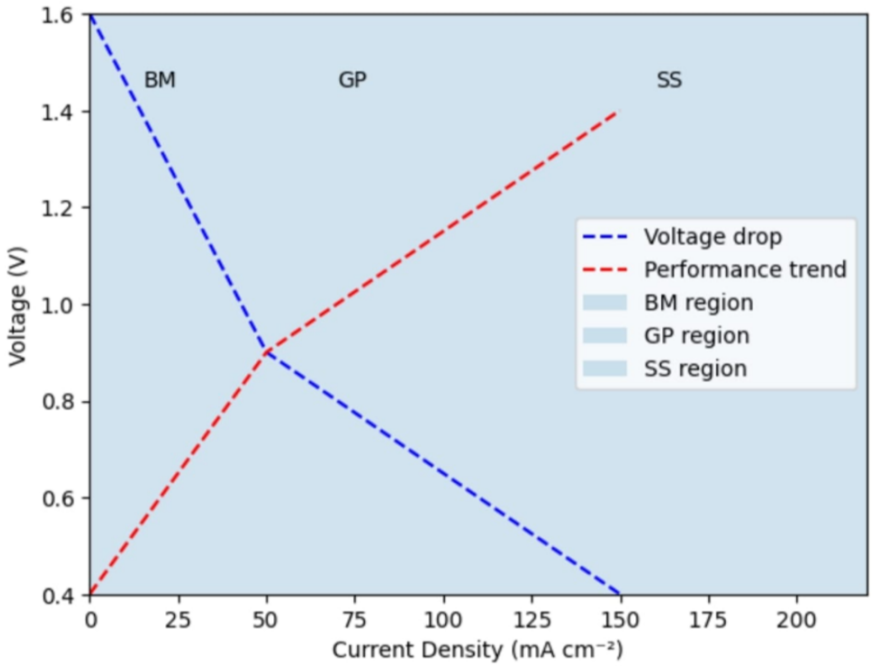

Figure 2. Colored polarization behavior illustrating voltage response across activation, ohmic, and mass-transport regions.

4.2. Electrochemical performance and efficiency analysis

Polarization curves and efficiency metrics demonstrated substantial performance variations (**Figure 1b** and **Table 1**). The internal resistance (R_0), calculated from the instantaneous voltage drop during pulse tests, remained consistent across all designs (~0.25 $\Omega \cdot cm^2$), confirming comparable ohmic losses. However, the mass transport limitations differed significantly. The SS design reached its limiting current at 140 $mA \cdot cm^{-2}$, while the BM and GP designs extended this to 175 $mA \cdot cm^{-2}$ and 190

$mA \cdot cm^{-2}$, respectively.

During charge-discharge cycling at 80 $mA \cdot cm^{-2}$, the BM design achieved the highest voltage efficiency (VE) of 84.2% and energy efficiency (EE) of 80.5%, outperforming the SS baseline (VE = 81.5%, EE = 77.8%). The GP design showed competitive performance with VE = 83.0% and EE = 79.8%.

4.3. Mass transport enhancement mechanisms

The superior performance of the advanced flow fields can be attributed to their distinct mass transport enhancement mechanisms. The BM design's branching architecture ensures more uniform reactant access to the entire electrode area, reducing concentration polarization through optimized distribution rather than intense local mixing. Conversely, the GP design creates controlled turbulence through vortex generation downstream of each micro-pillar, effectively disrupting concentration boundary layers and enhancing local mass transfer coefficients by up to 45% compared to the SS design.

This analysis reveals a fundamental design trade-off: while geometric perturbators provide superior local mixing and higher limiting currents, they incur greater pumping penalties. The biomimetic approach offers a more balanced solution, achieving significant performance improvements with minimal parasitic losses. These findings provide crucial insights for flow field optimization strategies tailored to specific application requirements, whether prioritizing maximum power density or overall system efficiency.

5. Conclusion

This study established and validated a hybrid calculation-estimation framework for the physics-based modeling and optimization of vanadium redox flow battery (VRFB) flow fields. The core methodological principle—prioritizing direct calculation of parameters from geometry or experiments over empirical estimation—was implemented in a 3D multi-physics model and served as a robust foundation for design analysis. The framework was deployed to systematically evaluate three distinct flow field paradigms: a conventional serpentine baseline, a biomimetic branching network inspired by leaf venation, and a serpentine channel augmented with passive geometric perturbators. The results demonstrate that the biomimetic design achieves an optimal balance, reducing pressure drop by 32% and increasing net system efficiency by 3.2% (absolute) over the baseline. This performance stems from its hierarchically branched, low-resistance architecture, which ensures superior electrolyte distribution with minimal parasitic loss. The perturbator-enhanced design, while achieving the highest limiting current density (190 $mA \cdot cm^{-2}$) via vortex-induced mixing, incurred a greater hydraulic penalty.

In summary, this work provides a validated modeling strategy and clear design guidelines. It establishes that moving beyond conventional layouts through nature-inspired engineering is a crucial pathway to developing more efficient and cost-effective VRFBs. For applications prioritizing overall system efficiency, biomimetic architectures are optimal, whereas designs enhancing local mixing are

better suited for high-power-density scenarios requiring maximum reactant utilization.

Author contributions: The author confirm contribution to the paper as follows: Conceptualization, JH and KKK; validation, JH, KKK and CH; formal analysis, JH and CH; investigation, JH, KKK and CH; resources, JH and KKK; data curation, CH and AK; writing—original draft preparation, JH, KKK and MB; writing—review and editing, JH, AK and MB; visualization, JH and MB; supervision, JH, AK and MB; project administration, AK and MB; funding acquisition, KKK. All authors have read and agreed to the published version of the manuscript.

Funding: This research was funded by the Deanship of Scientific Research of Taif University, grant number 83/Deanship-of-Scientific-Research, and the APC was funded by the Deanship of Scientific Research of Taif University (DSRTU).

Institutional review board statement: Ethical review and approval were waived for this study, as it did not involve human participants, animals, or sensitive personal data requiring formal oversight under the guidelines of Taif University.

Informed consent statement: Not applicable.

Data availability statement: The data that support the findings of this study are available from the corresponding author upon reasonable request. The flow field geometries and simulation parameters are described in sufficient detail within the article to allow for replication of the study.

Acknowledgments: The authors would like to acknowledge the Deanship of Graduate Studies and Scientific Research, Taif University, for funding this work.

Conflict of interest: The authors declare no conflict of interest.

References

1. Ali A, Ramadesigan V, Monder DS. Modelling and simulation based impact analysis of electrode parameters on the performance of vanadium redox flow batteries. Journal of Power Sources. 2025; 653: 237659. doi: 10.1016/j.jpowsour.2025.237659
2. Ren J, Wei L, Wang Z, et al. An electrochemical-thermal coupled model for aqueous redox flow batteries. International Journal of Heat and Mass Transfer. 2022; 192: 122926. doi: 10.1016/j.ijheatmasstransfer.2022.122926
3. Yifru BA, Lim KJ, Bae JH, et al. A hybrid deep learning approach for streamflow prediction utilizing watershed memory and process-based modeling. Hydrology Research. 2024; 55(4): 498–518. doi: 10.2166/nh.2024.016
4. Xiong B, Ding Y, Zhang Q, et al. Finite element-based analysis of composite serpentine flow channel 3D modeling of vanadium redox flow battery. International Journal of Green Energy. 2025; 22(5): 831–838. doi: 10.1080/15435075.2021.2007390
5. Chatterjee A. Investigation of self-excited induction generator for supporting domestic loads and its extension to a microgrid. Energy Storage and Conversion. 2024; 2(2): 1321. doi: 10.59400/esc.v2i2.1321
6. Liang G, Lin S, Hu W, et al. Joint Model Parameter Identification and Extended Kalman Filter Algorithm for the State of Charge Estimation of Lithium Iron Phosphate Battery. Journal of Electrochemical Energy Conversion and Storage. 2025; 22(3): 031010. doi: 10.1115/1.4066637
7. Schweidtmann AM, Zhang D, Von Stosch M. A review and perspective on hybrid modeling methodologies. Digital Chemical Engineering. 2024; 10: 100136. doi: 10.1016/j.dche.2023.100136
8. Cai W, Xiao L, Deng T, et al. Analysis of residual stress for thin-layered electrolyte co-sintered with porous electrodes applied in solid oxide cells. Thin-Walled Structures. 2025; 211: 113140. doi: 10.1016/j.tws.2025.113140

9. Kumar D, Rizwan M, Panwar AK. Robust state of health estimation of commercial lithium-ion batteries based on enhanced hybrid machine learning model for electrified transportation. Electrical Engineering. 2025; 107(4): 5053–5070. doi: 10.1007/s00202-024-02808-8
10. Guo L, Xu G. A Novel Hybrid Framework for Short-Term Carbon Emissions Forecasting in China: Aggregate and Sectoral Perspectives. Sustainability. 2025; 17(22): 10206. doi: 10.3390/su172210206
11. Sarwa B, Możdzierz M, Brus G. Artificial intelligence-based modeling of solid oxide fuel cells for improved transient prediction and control optimization. Journal of Power Sources. 2025; 658: 238281. doi: 10.1016/j.jpowsour.2025.238281
12. Ma Q, Shi H, Li H, et al. Topology optimization design of electrode integrated with flow field for intensifying reactive transfer process of non-aqueous iron-vanadium redox flow battery. Chemical Engineering and Processing—Process Intensification. 2025; 213: 110309. doi: 10.1016/j.cep.2025.110309
13. Kumar A, Dhanka S, Sharma A, et al. A hybrid framework for heart disease prediction using classical and quantum-inspired machine learning techniques. Scientific Reports. 2025; 15(1): 25040. doi: 10.1038/s41598-025-09957-1
14. Calborean A, Máthé L, Bruj O. Phase Change Materials for Thermal Management in Lithium-Ion Battery Packs: A Review. Batteries. 2025; 11(12): 432. doi: 10.3390/batteries11120432
15. Hu H, Han M, Liu J, et al. Strategies for improving the design of porous fiber felt electrodes for all-vanadium redox flow batteries from macro and micro perspectives. Energy & Environmental Science. 2025; 18(7): 3085–3119. doi: 10.1039/D4EE05556J
16. Wang Q, Shan X, Liu H, et al. Mass transfer in micro-nano porous electrodes: A crucial role in optimizing vanadium redox flow battery performance. Journal of Colloid and Interface Science. 2026; 705: 139465. doi: 10.1016/j.jcis.2025.139465
17. Yang WW, Bai XS, Zhang WY, et al. Numerical examination of the performance of a vanadium redox flow battery under variable operating strategies. Journal of Power Sources. 2020; 457: 228002. doi: 10.1016/j.jpowsour.2020.228002
18. Liu X, Pan L, Rao H, et al. A review of transport properties of electrolytes in redox flow batteries. Future Batteries. 2025; 5: 100019. doi: 10.1016/j.fub.2024.100019
19. Shoaib M, Vallayil P, Jaiswal N, et al. Advances in Redox Flow Batteries—A Comprehensive Review on Inorganic and Organic Electrolytes and Engineering Perspectives. Advanced Energy Materials. 2024; 14(32): 2400721. doi: 10.1002/aenm.202400721
20. Guo Z, Ren J, Sun J, et al. A split convection-enhanced flow field for stack-scale redox flow batteries. Chemical Engineering Journal. 2025; 511: 161937. doi: 10.1016/j.cej.2025.161937
21. Cheng Q, Li MJ, Wang RL, et al. Design and optimization of guide flow channel for vanadium redox flow battery based on the multi-field synergy. Journal of Power Sources. 2025; 650: 237526. doi: 10.1016/j.jpowsour.2025.237526
22. Huang Z, Liu Y, Xie X, et al. Design and optimization of a novel flow field structure to improve the comprehensive performance of vanadium redox flow batteries. Journal of Power Sources. 2025; 640: 236736. doi: 10.1016/j.jpowsour.2025.236736
23. Li X, Yuan C, Chen X, et al. Temperature-dependence of Zn deposition/stripping behavior in aqueous Zn-based flow batteries. Journal of Energy Chemistry. 2025; 107: 260–268. doi: 10.1016/j.jechem.2025.03.049
24. Basavaraju SK, Chavati GB, Sannaobaiah MB, et al. Investigation of $CeVO_4$-decoracated activated carbon-nanocomposite as a bifunctional electrode material for vanadium flow battery and supercapacitor applications. Composite Structures. 2025; 371: 119524. doi: 10.1016/j.compstruct.2025.119524
25. Agyekum EB, Abdullah M, Odoi-Yorke F, et al. A state-of-the-art review of electrolyte systems for vanadium redox flow battery—Status of the technology, and future research directions. Energy Conversion and Management: X. 2025; 27: 101180. doi: 10.1016/j.ecmx.2025.101180
26. Huang Z, Xuan L, Liu Y, et al. Numerical analysis of asymmetric biomimetic flow field structure design for vanadium redox flow battery. Future Batteries. 2025; 5: 100017. doi: 10.1016/j.fub.2024.100017